PHYSICAL REVIEW E, VOLUME 63, 055401(R)

Interface imprinting by a rippled shock using an intense laser

J. O. Kane,[1] H. F. Robey,[1] B. A. Remington,[1] R. P. Drake,[2] J. Knauer,[3] D. D. Ryutov,[1] H. Louis,[1] R. Teyssier,[4] O. Hurricane,[1] D. Arnett,[5] R. Rosner,[6] and A. Calder[6]
[1]*Lawrence Livermore National Laboratory, Livermore, California 94550*
[2]*University of Michigan, Ann Arbor, Michigan 48105*
[3]*Laboratory for Laser Energetics, University of Rochester, Rochester, New York 14623*
[4]*CEA, Saclay, France*
[5]*University of Arizona, Tucson, Arizona 94550*
[6]*University of Chicago, Chicago, Illinois 60637*
(Received 7 December 2000; published 26 April 2001)

Perturbation imprinting at a flat interface by a rippled shock has been observed in a laser hydrodynamics experiment. A strong shock was driven through a three-layer target, with the first interface rippled, and the second flat. The chosen thickness of the second layer gave instability growth with opposite phases at the two interfaces, consistent with two-dimensional simulations and rippled shock theory.

DOI: 10.1103/PhysRevE.63.055401 PACS number(s): 52.35.Tc, 47.20.−k, 47.40.−x

In a type II supernova, a strong radially expanding shock crosses from the collapsed core of the star into the overlaying layers [1]. Asphericities in the core, convection behind the shock during shock formation, and density perturbations in the layers above the core can distort the shock [2] and imprint perturbations at interfaces separating layers above the core. These interface perturbations can grow by the Richtmyer-Meshkov (RM) [3] and Rayleigh-Taylor (RT) instabilities [4] and affect the ejection of ^{56}Ni, produced in the O layer by explosive nuclear burning behind the shock. In inertial confinement fusion [5,6], multiple shocks are used to compress a fuel capsule, and shock-imprinted interface perturbations can strongly degrade the performance of the capsule.

In linear theory for compressible fluids, single-mode sinusoidal perturbations of wavelength λ on the shape of a planar shock front oscillate with an amplitude that decreases asymptotically as a power law with distance traveled, with exponent $-1/2$ for strong (high Mach number) shocks, and $-3/2$ for weak shocks (Mach number near 1) [7–9]. When the shock reaches a flat interface with a density step, the shock imprints a perturbation of wavelength λ on the interface. The growth rate and phase of the interface perturbation is determined predominantly by the longitudinal velocity perturbation of the shock at the moment the shock hits the interface, and is largest when the velocity amplitude is at a maximum [6]. We have performed experiments at the Omega laser at the University of Rochester [10] in which a perturbed planar shock imprints a perturbation at a material interface having a step down in density.

Figure 1 shows an exploded view of the target used for the Omega laser experiments. The target consists of three main layers of material in a cylindrical Be shock tube, with initial density decreasing in the direction the shock travels. The materials are Cu: polyimide plastic: carbonized resorcinol formaldehyde (CRF) foam, with thicknesses 85, 150, and 1700 μm and densities 8.93, 1.41, and 0.1 g/cm^3, respectively. The Be tube delays lateral decompression of the target, giving a more planar shock. The tube has an outer radius of 550 μm and an inner radius of 400 μm. For ease of target assembly, the section of the tube containing the Cu polyimide plug is bored out to inner diameter 475 μm. The surface of the Cu layer is machined with a sinusoidal ripple of wavelength $\lambda = 200\ \mu$m and amplitude $\eta_0 = 15\ \mu$m. A 10 μm CH ablator (density 1.05 g/cm^3) at the laser drive end of the target prevents direct illumination of the Cu and associated preheating of the rest of the target. Embedded within the polyimide layer is a tracer strip of CH(4.3 atomic % Br), with density 1.42 g/cm^3. The tracer strip is 75 μm thick perpendicular to the polyimide-foam interface and 200 μm thick parallel to the ripples on the Cu-polyimide interface. A 75 μm thick, 2.5 mm diameter Be shield (not shown) with a central aperture of 950 μm diameter is mounted at the front of the target.

The target is driven by ten beams of the Omega laser with a nominal measured energy of 420 J/beam in a 1 ns pulse at a laser wavelength $\lambda_L = 0.351\ \mu$m. The beams are smoothed by distributed phase plates [11], which determine the size of the beam spots. Six beams are incident on the ablator at an angle of 23.2° from the target normal, azimuthally oriented in a symmetric hexagonal array; four beams are incident at an angle of 47.8°. The spatial profile of each beam is a super-Gaussian with an intensity given by $I(\mathrm{W/cm^2}) = 8.9 \times 10^{13} \exp[-(r/412\ \mu\mathrm{m})^{4.7}]$. The peak intensity in the overlapped spot is 7.2×10^{14} W/cm^2, and the average intensity on the CH ablator over the 950 μm diameter is 5.7×10^{14} W/cm^2. Absorption of the laser light couples energy into the CH ablator at or below the critical electron density, and electron heat conduction carries some of this energy from the absorption zone to the ablation front. The laser ablation generates a hot, low density, high velocity ''exhaust plasma'' which, by reaction impulse, produces a strong, 35 Mbar shock transmitted forward into the Cu. The shock is perturbed is it crosses the Cu-polyimide interface, and oscillates until it reaches the polyimide/CH(Br)-foam interface, where it imprints a perturbation. Both interfaces are observed side-on with hard x-ray radiography, using a gated framing camera [12]. Eight additional Omega beams are focused onto a 12 μm thick Fe backlighter foil located 4 mm from the target, generating 6.7 keV x-rays to which the Cu and the

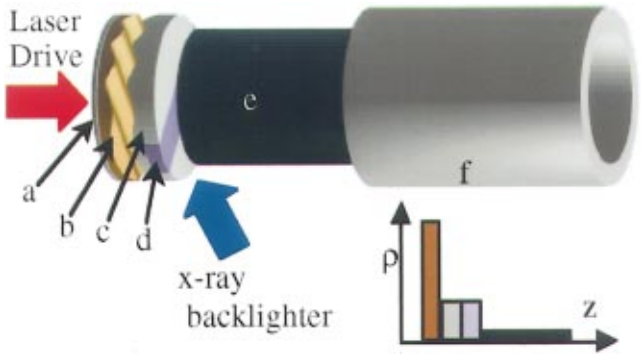

FIG. 1. (Color). Exploded view of the target. (a) CH, (b) Cu, (c) polyimide, (d) CH(Br), (e) foam, (f) Be tube. Inset: schematic density.

CH(Br) tracer strip are opaque, and the polyimide and foam nearly transparent. Nearly all of the contrast at the polyimide/CH(Br)-foam interface comes from the tracer layer, allowing visualization of the shock-imprinted structure at that interface over only the central 200 μm of the target along the line of sight, without edge effects near the wall of the shock tube.

We use several hydrodynamics codes to design and simulate the experiments. The first is HYADES, a one-dimensional (1D) code with laser deposition, radiation transfer, heat conduction by electrons, average atom ionization, and tabular equation of state (EOS) [13]. The second code used is CALE, which has 2D planar or *r-z* axisymmetric geometry, arbitrary Lagrangian-Eulerian hydrodynamics, interface tracking, and tabular EOS [14]. We have also done 2D simulations with the astrophysics code PROMETHEUS [15]. While astrophysical simulations with PROMETHEUS have used complex equations of state, these new PROMETHEUS simulations are the first using tabular EOS for laser experiments; previous work used ideal gas EOS [16,17]. We model the input of laser energy in HYADES, allowing the shock to form and cross the flat CH ablator and Cu layer. At time $t=2.1$ ns, when the shock is about to reach the valley of the 2D perturbation at the Cu-polyimide interface, we map density, velocity, and temperature or pressure into the 2D codes, and impose the perturbation at the Cu-polyimide interface. Due to the lack of an accurately determined EOS for the foam [18], we use an ideal gas EOS with fixed isentropic exponent $\gamma=1.286$, which reproduces the observed shock speed in the foam. After the mapping time, the problem is purely hydrodynamic, due to the relatively high densities and low temperatures involved. This was confirmed by running CALE with heat conduction by electrons and radiation turned on or off in different simulations. In the 2D simulations, we use planar geometry, because the Cu-polyimide ripple is 2D, but the cylindrical shock tube introduces 3D edge effects. We have simulated the purely axisymmetric problem having no perturbation at the Cu-polyimide interface in both cylindrical and planar geometry, and found less than a 5% difference in the interface and shock velocities, and little qualitative difference in the planarity of the shock.

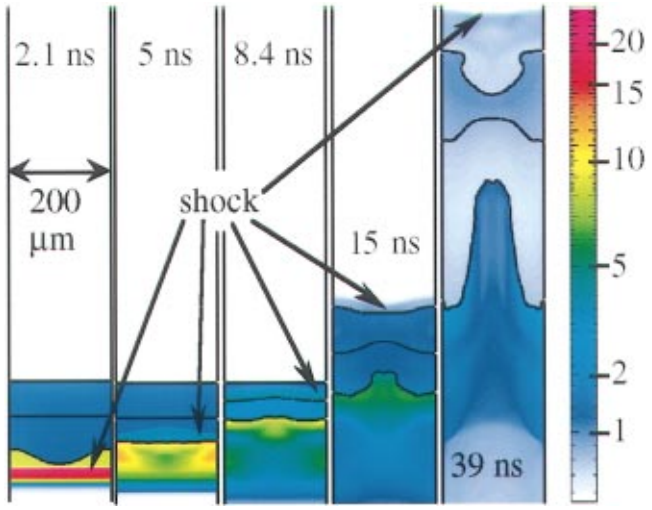

FIG. 3. (Color). CALE simulation of one half wavelength of perturbation. From bottom: heavy lines separate Cu, polyimide, CH(Br), foam. Density scale at right is in g/cm^3.

In Fig. 2 we show how the shock oscillates with distance Δz traveled in the polyimide, from a simplified 2D CALE simulation of the experiment in which we model only the Cu

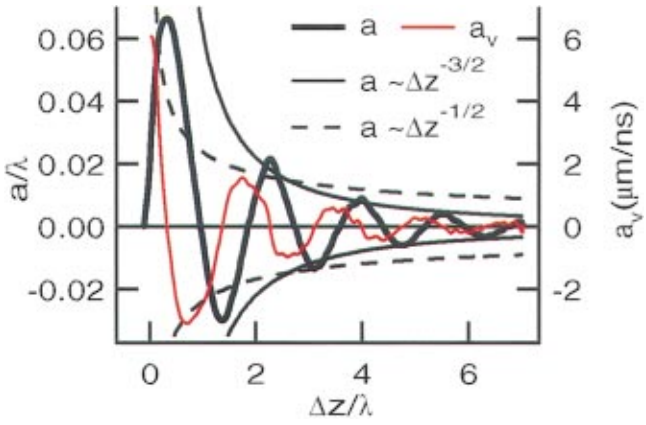

FIG. 2. (Color). Spatial (a) and velocity (a_v) amplitudes of shock perturbation vs Δz.

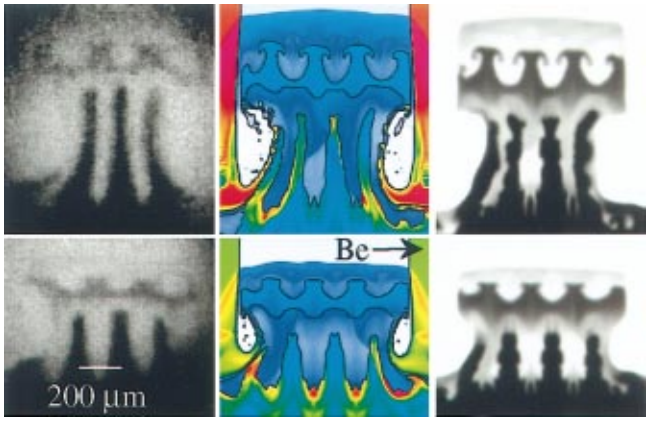

FIG. 4. (Color). Data and simulations. Bottom: $t=39$ ns. Top: $t=65$ ns. Left: data. Middle: CALE density. Right: simulated radiograph of PROMETHEUS results.

and a thick polyimide layer, with no foam layer or Be tube. We model one half wavelength of the perturbation, using reflecting boundaries in the lateral direction. The heavy oscillating line is the spatial amplitude a of the shock and the light oscillating line is velocity amplitude $a_v = da/dt$. We take Δz as the distance between the initial average Cu-plastic interface position and the average shock position, and a as the peak-to-valley amplitude. We note that a inverts by $\Delta z/\lambda \approx 1$ and again by $\Delta z/\lambda \approx 2$. Because a is decaying with Δz, $|a_v|$ reaches a local maximum not at $\Delta z/\lambda \sim 1$ but at $\Delta z/\lambda \sim 0.75$, i.e., $\Delta z = 150\ \mu$m. CALE simulations which include the foam layer predict stronger imprinted growth for $\Delta z = 150\ \mu$m than for $\Delta z = 200\ \mu$m. These results are consistent with a_v determining the phase and amplitude of the imprinted perturbation [6], but the full interaction of the spatial and velocity amplitudes and the role of nonlinear effects require further investigation. Finally, although the Mach number of the shock is greater than 5, a weak-shock fit, $a \sim \Delta z^{-3/2}$ (solid line in Fig. 3), is much better than a strong-shock fit, $a \sim \Delta z^{-1/2}$ (dashed line). This suggests that overall decompression of the target may affect the shock stability, at least asymptotically, for $\Delta z \gg \lambda$. Analytic theory describing the imprinted perturbation has been done for the asymptotic regime [6], whereas imprinting in the experiment occurs at $\Delta z < \lambda$. We will continue our analysis of the shock oscillation and imprinting elsewhere.

Figure 3 illustrates the hydrodynamics of the experiment, again from a simplified 2D CALE simulation, but now including the CH(Br) tracer and the foam layer. The thickness of the polyimide CH(Br) layer is $\Delta z = 150\ \mu$m. We again model only one half wavelength of the perturbation; for clarity we reflect the result across $r = 0$ in each panel of Fig. 3. The field of view is $z = 0$ to 1000 μm, with the initial back side of the CH ablator at $z = 0\ \mu$m. At the mapping time, $t = 2.1$ ns, the planar shock is clearly visible approaching the Cu-polyimide interface. By $t = 5$ ns a perturbed transmitted shock has entered the polyimide and a reflected rarefaction is moving back through the Cu. The RM instability has partly inverted the Cu-polyimide interface, which is now decelerating and RT unstable, because the gradients of pressure and density are opposed there. By $t = 8.4$ ns, the Cu-polyimide interface is almost fully inverted, and the shock is about to reach the CH(Br)-foam interface. The shock has oscillated to reduced spatial amplitude, and the amplitude of the velocity perturbation on the shock is approaching a maximum, consistent with Fig. 2. By $t = 15$ ns the shock has crossed the CH(Br)-foam interface and imprinted a velocity perturbation in phase with the velocity perturbation of the shock at the crossing time; that interface is now RT-unstable. Meanwhile, a reflected rarefaction has moved back through the polyimide/CH(Br) layer and reaccelerated the rippled Cu-polyimide interface, where density and pressure gradients are no longer opposed. By $t = 39$ ns the perturbation at the CH(Br)-foam interface has grown, with the ''bubble'' of foam rising towards the falling spike of Cu. The Cu spike is greatly elongated by the rarefaction. CALE simulations with $\Delta z = 2\lambda = 400\ \mu$m predict in-phase growth, with the bubble of foam rising towards the bubble of polyimide. In this case, the additional effect of the Cu spikes directly perturbing the CH(Br)-foam interface could ostensibly produce in-phase growth. Thus, in order to unambiguously demonstrate shock imprinting experimentally, we used targets with $\Delta z = 150\ \mu$m, to give out-of-phase growth.

In Fig. 4 we show results from the experiment. The top and bottom panels are for times $t = 39$ and 65 ns, respectively. The left panels are side-on radiographs from the experiment, the middle panels shows density from the CALE simulation, and the right panels show the PROMETHEUS results as simulated radiographs; simulated radiographs of the CALE results look very similar (not shown). For $t = 39$ ns, the field of view is $z = 250$ to 1100 μm and $r = -500$ to 500 μm, with the axis of the tube at $r = 0\ \mu$m. For $t = 65$ ns, the field of view is $z = 450$ to 1100 μm and $r = -500$ to 500 μm. In the simulations, we model the full target, including the Be tube and washer. Both 2D simulations are run on the same fixed Cartesian grid. The resolution in the simulations is approximately 4 μm per zone but with finer resolution in the z direction near the Cu-polyimide interface to represent the initial interface ripple more accurately. The resolution is coarser in the r direction in the Be tube and washer, where higher accuracy is not needed. The agreement between the data and codes is very good. The long dark ''fingers'' in the data are spikes of Cu expanding in the rarefaction reflected from the CH(Br)-foam interface; bubbles of polyimide separate the spikes. The horizontal strip of opaque material above the Cu spikes is the CH(Br) tracer. We can easily see imprinted growth at the CH(Br)-foam interface. The CH(Br) spikes are out of phase with the Cu spikes, as expected. The shape of the CH(Br)-foam interface is reproduced reasonably well in the simulations.

Other features are available in the data for benchmarking simulations. In the simulations, dense shock compressed foam and the shock itself are visible above the tracer strip; the shock is faintly visible in the data. The inner part of the Be tube wall is visible in the CALE simulation in Fig. 4. In the data, the inner walls of the transparent tube are marked by the sharp edges at the left and right of the CH(Br). At left and right in the CALE simulation, a large vortex ring of tube material and entrained foam is visible bulging from the inner tube wall into the polyimide; its inner edge is faintly visible in the data. At the base of the Cu spikes, the Cu and the Be tube are blowing out laterally. In the data, a left-right asymmetry in the Cu spikes is evident; it is due to the tube axis passing between a valley and a peak of the initial machined perturbation. The codes reproduce the asymmetry. In the data, a smaller distorted spike of Cu is visible on the left, near the vortex ring. This spike appears longer in the simulations. In the true geometry, this spike grew from a short ripple parallel to the nearby tube wall; thus, it is subject to 3D effects which are not simulated, and furthermore has low optical depth in the data. In the full set of data, to be reported elsewhere, several radiographs show the shock, the shock compressed foam, and edge of the vortex ring very clearly, and the simulations are in agreement with these data. PROMETHEUS shows more fine structure along the Cu-polyimide interface than CALE; such fine structure is not well resolved in the data. PROMETHEUS has intrinsically higher resolution [17], as also suggested by the finer detail in the

spike tip rollups at the CH(Br)-foam interface. The interface tracking in CALE may also suppress fine structure.

We do not yet have a satisfactory *a priori* model of the fully 3D laser drive. In HYADES we treat the overlapped beams simply as a single beam incident normal to the surface; preliminary 2D simulations in CALE suggest that using multiple beams with non-normal incidence does not change the result significantly. However, if we use the full nominal laser intensity in HYADES, the interface and shock velocities in CALE are too high. For the simulations in Fig. 4, we used an *ad hoc* drive with a constant intensity of $3.5 \times 10^{14}\,\mathrm{W/cm^2}$ across the face of the plug, thus delivering 65% of nominal energy to the plug. This drive reproduced the observed gross 1D and 2D hydrodynamics, as determined by the velocities of the shock and the interfaces, and by other features discussed above. Also, if we map into the 2D codes from multiple 1D HYADES simulations having laser intensity that varies spatially with the true radial intensity profile, the shock is noticeably more bowed in the simulation than in the data. Using constant intensity across the plug produced a more planar shock, in better qualitative agreement with the data.

We have successfully produced perturbation imprinting by an oscillating shock in a laser hydrodynamics experiment, using a three-layer Cu-polyimide/CH(Br)-foam target in a shock tube, and have observed behavior qualitatively consistent with theory for a rippled shock. The hydrodynamics studied are relevant to type II supernovas and to inertial confinement fusion. A planar shock was perturbed by a single mode sinusoidal perturbation at the heavy-to-light Cu-polyimide interface, resulting in an oscillating shock that imprinted a perturbation at the initially flat, heavy-to-light CH(Br)-foam interface. By carefully choosing the thickness of the polyimide, we were able to produce instability growth with opposite phases at the two interfaces, indicating that perturbation growth on the second interface was seeded by the passage of a rippled shock. Hydrodynamic simulations were in very good agreement with the data. Oscillation of the shock is evident in the simulations, and the phase and amplitude of the imprinted perturbation on the initially flat interface appear to be determined by the velocity perturbation on the shock.

This work was performed under the auspices of the U.S. Department of Energy by University of California Lawrence Livermore National Laboratory under Contract No. W-7405-Eng-48.

[1] J. Kane *et al.*, Astrophys. J. **528**, 989 (2000).
[2] G. Bazan and D. Arnett, Astrophys. J. **496**, 316 (1998); K. Kifonidis, T. Plewa, H.-Th. Janka, and E. Mnller, *ibid.* **531**, L123 (2000).
[3] R. D. Richtmyer, Commun. Pure Appl. Math. **13**, 297 (1960); E. E. Meshkov, Izv. Akad. Nauk SSSR Mekh. Zhidk., Gaza **4**, 151 (1969) [Izv. Acad. Sci. USSR Fluid Dynamics **4**, 101 (1969)].
[4] S. Chandrasekhar, *Hydrodynamic And Hydromagnetic Stability* (Clarendon, Oxford, 1961).
[5] T. Endo *et al.*, Phys. Rev. Lett. **74**, 3608 (1995); R. J. Taylor *et al.*, *ibid.* **76**, 1643 (1996).
[6] R. Ishizaki *et al.*, Phys. Rev. E **53**, 5592 (1996).
[7] S. P. Dyakov, Zh. Eksp. Teor. Fiz. **27**, 288 (1954).
[8] L. D. Landau and E. M. Lifshitz, *Fluid Mechanics*, 2nd ed. (Pergamon Press, Oxford, 1987).
[9] N. C. Freeman, Proc. R. Soc. London, Ser. A **228**, 341 (1955).
[10] J. M. Soures *et al.*, Phys. Plasmas **3**, 2108 (1996); T. R. Boehly *et al.*, Rev. Sci. Instrum. **66**, 508 (1995); D. K. Bradley *et al.*, Phys. Plasmas **5**, 1870 (1998).
[11] Y. Lin, T. J. Kessler, and G. N. Lawrence, Opt. Lett. **20**, 764 (1995).
[12] H. F. Robey, K. S. Budil, and B. A. Remington, Rev. Sci. Instrum. **68**, 792 (1997); K. S. Budil *et al.*, *ibid.* **67**, 485 (1996).
[13] J. T. Larsen and S. M. Lane, J. Quant. Spectrosc. Radiat. Transf. **51**, 179 (1994).
[14] R. T. Barton, *Numerical Astrophysics*, edited by J. M. Centrella, J. M. LeBlanc, and R. L. Bowers (Jones and Bartlett Publishers, Inc., Boston, 1985), pp. 482–497.
[15] D. Arnett, B. A. Fryxell, and E. Müller, Astrophys. J. **341**, L63 (1989).
[16] J. Kane *et al.*, Phys. Plasmas **6**, 2065 (1999).
[17] R. L. Holmes *et al.*, J. Fluid Mech. **389**, 55 (1999).
[18] G. Hazak *et al.*, Phys. Plasmas **5**, 4357 (1998).